Case Studies in Construction Materials 15 (2021) e00741

Contents lists available at ScienceDirect

Case Studies in Construction Materials

journal homepage: www.elsevier.com/locate/cscm

Pet fiber reinforced sand performance under triaxial and plate load tests

José Wilson dos Santos Ferreira [a,1,*], Phillipe Campello Senez [b], Michéle Dal Toé Casagrande [a,2]

[a] Civil and Environmental Engineering Department, University of Brasilia, Brasilia, Federal District, 70910-900 Brazil
[b] Civil and Environmental Engineering Department, Pontifical Catholic University of Rio de Janeiro, Rio de Janeiro 22453-900, Brazil

ARTICLE INFO

Keywords:
Reinforced soil
Polyethylene terephthalate
Plastic waste
Triaxial tests
Laboratory scale model tests

ABSTRACT

Annually, large amounts of waste Polyethylene Terephthalate (PET) bottles are discarded worldwide, although their properties can be useful in engineering works, such as soil improvement. Thus, the influence of PET fibers on sandy soil mechanical behavior was assessed in the present work. Consolidated-drained triaxial tests were performed using a 0.5% addition of 1.4 (SF-1) and 3.3 dtex fibers (SF-2). Afterward, plate load and slopes tests in the laboratory scale model were carried out for the most effective fiber. Overall, the inclusion of both fibers improved the stress-strain behavior, evident by greater absorbed strain energy in the reinforced soil. The insertion of 1.4 dtex PET fibers enhanced the internal friction angle of the soil from 31.9° to 44.3°, while a 29.7° value was obtained from 3.3 dtex fibers. Also, a cohesion intercept portion was identified in both composites, corresponding to 22.5 and 58.7 kPa for SF-1 and SF-2, respectively. The PET reinforcement reduced both vertical and horizontal deformation and altered the soil failure mechanism. The settlement reduction in fiber-reinforced sand is stress magnitude dependent, decreasing about 81% for stresses above 300 kPa, in which settlement of 125.3 mm from unreinforced sand was reduced to 23.6 mm by fiber insertion at 400 kPa. At the maximum comparable settlement, a 375.7% enhancement was seen in the bearing capacity, increasing from 240 kPa to 1141.6 kPa. In addition to a better understanding of soil-PET mixture, the results contribute to encouraging sustainable applications in engineering, such as embankment, shallow foundation, and retaining wall layers.

1. Introduction

The excessive consumption of natural resources associated with large amounts of solid waste materials production is causing serious socio-environmental impacts and the land requirement for disposal, wherein the solid residues incorporation in production cycles becomes a solution to achieve sustainable development [1–5]. Globally, plastic waste generation exceeds 300 million tons annually, with an increasing rate of 4% per year [6]. In Brazil, only 1.2% of 11.3 million tons generated are recycled, and polyethylene

* Corresponding author.
E-mail addresses: ferreira.jose@aluno.unb.br (J.W.S. Ferreira), phill.senez@aluno.puc-rio.br (P.C. Senez), mdtcasagrande@unb.br (M.D.T. Casagrande).
[1] ORCID: 0000-0002-9675-9884.
[2] ORCID: 0000-0002-4740-0891.

https://doi.org/10.1016/j.cscm.2021.e00741
Received 31 July 2021; Received in revised form 10 October 2021; Accepted 11 October 2021
Available online 12 October 2021

represents 48.9% of all thermoplastic polymers discarded, with recycling been identified as the most effective plastic waste management strategy [7,8].

Polyethylene terephthalate (PET), a semi-crystalline thermoplastic polymer, due to the mechanical, chemical and thermal properties and production cost relationship, is one of the most produced plastics of the last two decades, resulting in large amounts of waste PET, because of its non-biodegradable nature and short-term usage [4,9,10]. Considering that plastic has satisfactory features (low density, high tensile strength, lightweight, and low cost), several studies have been conducted to evaluate plastic waste in engineering works, such as soil improvement.

Investigating sand reinforced with natural and synthetic fibers, Gray and Ohashi [11] reported bilinear failure envelopes related with a critical confining stress, also identified by Consoli et al. [12] under distinct stress paths. Benson and Khire [13] demonstrated the importance of the aspect ratio of high-density polyethylene (HDPE) strips inclusion on shear strength of sand soil. Improvements on tensile strength by adding plastic polystyrene in sand soil were reported by Ahmed [14], in agreement with findings of Consoli et al. [15], Park [16], Fatahi et al. [17] and Dhar and Hussain [18], using waste plastic fibers with a stabilized agent. From distinct PET size and content, Louzada et al. [4] demonstrated at low confining stress that the inclusion does not fill all the voids in the clayey soil, affecting the interaction between the materials and minimizing the soil load capacity. Based on previous research, variables such as form (e.g. powder, crushed and fibers) and aspect ratio of the inclusion, mixture proportion, type of soil and confining stress magnitude exert a high-level influence on the mechanical behavior of plastic waste reinforced soils [13,19–30].

One of the main concerns of fiber reinforcement is related to the fiber's orientation during the mixing and compaction process, which has been shown to result in non-isotropic mixture by Diambra et al. [31]. In this regard, both moist tamping and vibration procedures for preparing reinforced specimens lead to sub-horizontal orientation of fibers. The use of moist tamping technique to prepare specimens has the advantages of density control of the sample, prevention of fiber segregation and resemblance with the soil-fiber fabric generated in the field compaction [32–34]. Beyond that, the anisotropic behavior of fiber-reinforced sand was investigated by Ghadr and Bahadori [35] under undrained torsional shear tests, using a hollow cylindrical torsional shear apparatus, and they observed that sand particle shape plays a major role in fibers contribution to shear strength. Further, the increase in sphericity and roundness ratios of the particles reduced the anisotropy occurrence in specimen.

Evaluating the load-settlement response of fiber-reinforced sand in load plate tests, Consoli et al. [36,37] demonstrated that the bearing capacity and stiffness of the composite material are dependent on relative density and that the effect is more pronounced for higher densities. Mirzababaei et al. [38] studied the waste carpet fiber content and footing edge distance ratio influence on the behavior of slope under surface loading, obtaining bearing resistance improvements of 145%. Sotomayor and Casagrande [39] reduced the settlement, the number, and size of cracks propagation by adding coconut fibers randomly distributed under plate load tests.

Even though the importance of field tests to verify the mechanical behavior of the results obtained in laboratory tests, this practice tends to be uncommon in fiber-reinforced soils area, and laboratory scale model tests appear as a satisfactory solution for geotechnical applications. Nevertheless, there are few available studies, leading to a gap on PET fibers in geotechnical application [36–38]. In recognition of these needs, this study was conducted to achieve the goals: (1) evaluate the influence of different aspect ratio of waste PET fiber on sandy soil mechanical behavior, from triaxial tests; and (2) verify the contribution of the most efficient fiber on bearing capacity of the sand, by load plate and slopes tests in the laboratory scale model. The present research expects to contribute to a better understanding of soil-PET mixture and to encourage sustainable applications in engineering, and based on several limitations of it, theuse of higher confining stresses in triaxial tests, the replication of the experimental program considering distinct relative density of the composite, and the correlation of the results reported here with field test are suggested as possible future areas of study.

2. Experimental program

2.1. Materials

The materials used in this research were a poorly graded sand soil (Fig. 1a) extracted from Itaboraí – Rio de Janeiro/Brazil, and Polyethylene Terephthalate (PET) fibers obtained through the recycling of PET bottles. Fibers with distinct geometric features were selected, with textile title, diameter (d_f) and length (l_f) of 1.4 dtex, 0.0098 mm, and 38 mm (Fig. 1b) and 3.3 dtex, 0.023 mm, and 56 mm (Fig. 1c), respectively, resulting in fiber aspect ratios (l_f/d_f) of 3877 and 2435. It is important to point out that the textile title of the fiber is a linear measurement based on weight by unit length (1 dtex = 1 g/10,000 m). The fiber's specific gravity, determined by automatic gas pycnometer, is 1.21 g/cm^3, presenting 81 MPa tensile strength, 2800 MPa modulus of elasticity, and elongation at break of 70% [40].

The particle size distribution and properties of sandy soil is presented in Fig. 2 and Table 1 [41]. The chemical characterization by X-ray fluorescence analyzer showed the presence of Si (66.02%), Al (30.01%), K (3.20%), Ti (0.50%), and Fe (0.21%) in the soil, in agreement with the mineral composition identified from X-ray diffraction, consisted mainly by quartz grains (SiO_2), with low degree of sphericity and roundness, and high angularity, indicating small or no transport of the material.

2.2. Specimen preparation

Based on the similarity of the reinforcement mechanism presented by synthetic, natural and waste fibers, and considering the low specific gravity of PET fibers, the fiber addition of 0.5% in relation to the dry weight of the soil was employed, randomly distributed in the soil matrix [12,42]. Amounts above of 0.5% resulted in a visually non-homogeneous medium, since the large fibers' volume generates the fiber-fiber contact, which directly affected the grain-fiber reinforcement mechanism [28,33,43]. The abbreviation S100,

(a)

(b)

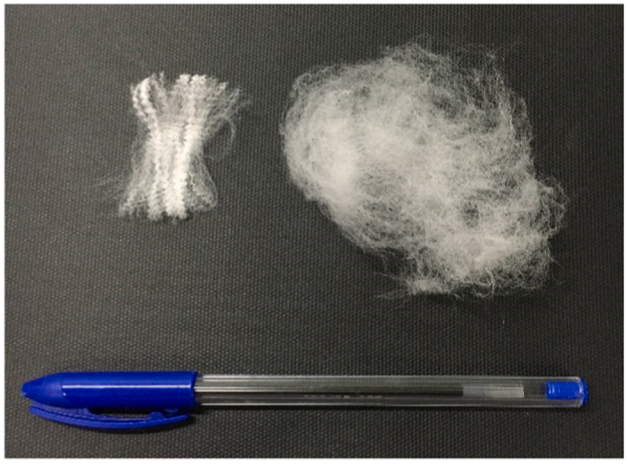

(c)

(caption on next page)

Fig. 1. Materials used in this research: (a) Sand soil; PET fiber (b) 1.4 dtex; (c) 3.3 dtex.

SF-1 and SF-2 refer, orderly, to sand and sand-PET fiber mixture with 1.4 and 3.3 dtex.

The moisture content of 10% was established from previous test, with the view to prevent excessive water in molding. The 50% relative density of sand (void ratio equals to 0.80) was defined for both unreinforced and reinforced soil, due to the lack of a standard to determine maximum and minimum void ratios for fiber reinforced sand, and it is consistent with the literature [24,36,37,39,44,45].

2.3. Testing methods

Consolidated-drained triaxial tests were carried out for non-reinforced sand and sand-PET fiber composites at the effective stress of 50, 100, and 150 kPa, to determine the stress-strain behavior and the strength parameters for superficial geotechnical applications, i.e., works limited to confining stresses up to 150 kPa, which can include embankments, shallow foundation placed in the reinforced layers of soil, and retaining wall layers. The mixtures were prepared by manually mixing the dry soil, PET fibers (when applicable), and water, preventing the entanglement process that occurs when fibers entangled with each other and separate from the matrix, thus ensuring the uniformity of the mixture. The specimens were made by static compaction directly onto the triaxial press pedestal, controlling the height of each of the three layers into which the mold was divided during the compaction, based on the moist tamping technique [31–34,38]. The specimen presented height and diameter of 8.6 cm and 4.0 cm, respectively.

The samples were saturated using backpressure and water percolation. Skempton's parameter B value equal to or greater than 0.95 was considered acceptable [46]. To avoid any pore pressure excess during the shear phase, the criterion present in Head [47] was employed, leading to a rate of 0.030 mm/min.

The tests were performed using conventional triaxial with strain-controlled test, presenting a capacity of 10 t. The load cell used has a maximum capacity of 5000 kN and an accuracy of 0.1 kN. The displacement was quantified using linear variable displacement transducer (LVDT) with 25 mm of course and accuracy of 0.01 mm. The measurements of the pressure in chamber, the volume gauge, and the pore pressure occurred by transducers with a range between 2 kPa and 1700 kPa. The volume change was obtained through the volumetric variation measurer (VVM), manufactured in PUC-Rio, following the Imperial College model.

The plate load and slope tests were conducted in a laboratory physical model with the non-reinforced sand and most efficient composite, based on triaxial tests. To simulate a continuous medium without interference from the side walls and the bottom of the box, using a rigid circular steel plate 10 cm in diameter and 2.54 cm thick, a box consisting of four high density wood plates and an acrylic sheet, with 80 cm in length, and 60 cm in width was designed. According to the criteria that the stress bulb generated by the plate load test only represents the characteristics of the soil up to two diameters below the plate, a depth of 45 cm was defined for the box [48]. The ratio of the plate diameter to mean particle size (D_{50} = 0.59 mm) is near to 170—i.e., above 50—which ensures that there is no effect for the model plate size on the bearing capacity, as reported by Toyosawa et al. [49]. The buckling of the walls was avoided using lateral reinforcement composed of steel profiles. To assurance the homogeneity and relative density of 50%, the materials were mixed using a rotary drum mixer. First, the dry soil and fibers were mixed, and then the water was added in parts until reaching the required amount. The box was divided into four layers of 0.1 m each for compaction.

During the plate load tests, the vertical displacements that occurred around the plate were measured by three displacement transducers type with a stroke of 100 mm arranged at 5, 7.5 and 10 cm of the plate edge (Fig. 3), intending to evaluate the soil behavior around the plate and its rupture mode. For the slope, an angle of 45° was selected for the tests, in agreement with executive

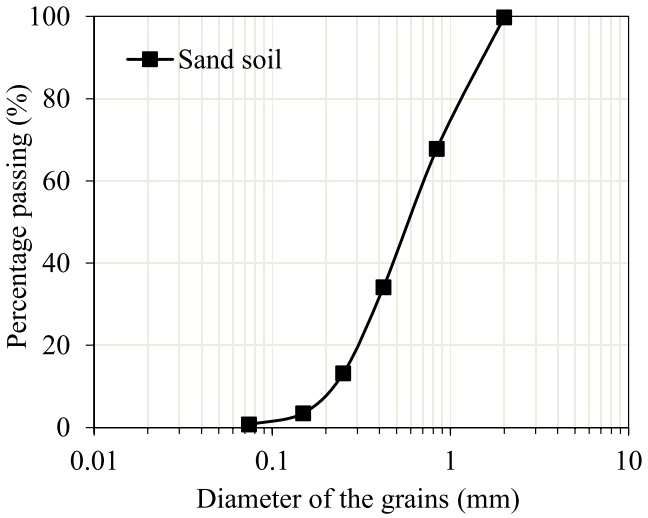

Fig. 2. Sandy soil particle-size distribution curve.

recommendation for slope in sandy soils on highways in Brazil. The slope was built using aluminum parts designed and molded for this purpose. The displacement transducers were positioned horizontally on the top, middle, and bottom of the slope (Fig. 4) to measure the horizontal displacements caused by the increase in load. The plate center was placed at a distance of approximately 13.5 cm from the edge of the slope, leading to a ratio of the distance between nearest edge of the plate and the crest of the slope equal to 0.85. Introduced by Mirzababaei et al. [38], the authors have shown that the edge of the plate to the slope-crest distance from 0 to 3 times the plate diameter does not cause significant variation in the results.

The rigid circular steel plate was coupled to the MTS load system, consisting of a universal reaction frame attached with a hydraulic servo actuator and a 100 kN load cell. The plate displacement was monitored by an internal data acquisition system connected to the actuator, which directly measures the displacement of the loading cell. Another external data acquisition system was connected to the displacement transducers. The load application occurred in a controlled manner at 0.2 kN/s rate [50].

3. Test results and analysis

3.1. Conventional triaxial tests

3.1.1. Stress-strain-volumetric results

The stress-strain-volumetric response obtained through CID triaxial tests for sand and sand-PET fiber composites is presented in Fig. 5. The inclusion of PET fibers caused an increase in resistance as the effective stress increased. Compared to non-reinforced sand, an increment in the maximum deviatoric stress is observed for both PET fiber composites, which suffered a hardening effect with the increase in axial strain (strain-hardening).

By analyzing the fiber-reinforced sand, the SF-1 mixture demonstrated superior stress-strain behavior. For the same mixture ratio, SF-1 contains finer and smaller fibers (1.4 dtex and 38 mm length) and, consequently, lighter—resulting in a greater number of filaments within the soil matrix, when compared to 3.3 dtex PET fibers. Thus, the randomly distributed presence of these fibers is more likely to pass through the soil rupture surface [14,27].

The volumetric strain ε_v vs. ε_a curves demonstrated a compressive nature for all the experimental conditions, indicating that the fiber adding does not modify the non-reinforced sand tendency, as observed by Consoli et al. [36] and Louzada et al. [4]. At approximately 2% axial strain, a parallel behavior is observed between the stress-strain curves fiber-reinforced soil, where curves increasing accompanied by the widen in effective confining stresses applied. This behavior is believed to occur on account of a single strength increase rate existence with the axial strain from the moment the fibers are mobilized. Also, this contribution remains visible until the axial strain limit of 18%.

3.1.2. Shear strength parameters

The effect on the strength parameters incurred by the fiber inclusion is shown in Fig. 6. It is seen that the PET addition caused an improvement in cohesion intercept for both composites, ranging from 0 to 22.51 kPa (SF-1) and 58.77 kPa (SF-2). In respect of the internal friction angle of the sand (31.97º), an increment of 38.7% was obtained by SF-1 (44.33º), while SF-2 suffered a short reduction (29.72°). It has been shown by many authors that a bilinear failure envelope in respect of fiber reinforced sand [12,13,51]. Under lower-pressure part of the failure envelope, as the present work, reinforcing mechanism is governed by fiber stretching and slippage, leading to significant gains in the internal friction angle, mainly, which agrees with the obtained results for sand-PET fibers with 1.4 dtex. Considering that fibers in fiber-reinforced sand in reality work in tension and not in shear [37,52–54], it is expected that the smaller aspect ratio presented by fibers with 3.3 dtex affected the mobilization of tension, in accordance with He et al. [55].

Considering the 50% relative density leading to an initial loose sand behavior, the 3.3 dtex fibers, with both larger diameter and length (0.023 mm and 56 mm, respectively), is expected to present superior mobilization stress in the presence of effective confining stresses higher than the 150 kPa used in this study. Under a low confining stress, the fiber's major role regards to gains in cohesion intercept, in the same way observed for polypropylene fibers.

The recommended relationship of fiber length (l_f) to the diameter of the matrix grains (D_{50}), $10 < Lf/D_{50} < 100$, established to fiber-reinforced sand by Diambra and Ibraim [29], was satisfied by both fibers SF-1 (64.4) and SF-2 (94.9). Although it was expected that the higher relation would result in greater interaction and, consequently, superior shear strength parameters, it is important to clarify that the length and diameter of the fiber varied in the present study, affecting the establishment of a simple correlation between the ratio and mechanical behavior. Further, not only the mean particle size, but also the grain shape parameters, affects the interaction mechanisms [35].

Table 1
Properties of the sand.

Property	Value
Specific gravity (Gs)	2.65
Effective size (D_{10}), mm	0.24
Uniformity coefficient (Cu)	2.90
Gradation coefficient (Cc)	1.0
Minimum void ratio (e_{min})	0.67
Maximum void ratio (e_{max})	0.93
USCS Classification	SP

3.1.3. Strain energy absorption capacity

Tenacity is the property of the material that expresses the energy absorbed by it when deformed. In this study, tenacity was assessed by the strain energy absorption capacity (Edef), which is a quantity numerically equal to the area under the stress × variation strain curve, evaluated up to an axial strain of 18%. Fig. 7 shows the variation in the strain energies absorbed under the different effective stresses applied.

The inclusion of PET fibers in the sand matrix demonstrated a non-linear increase in absorbed energy for all studied stress conditions. This beneficial effect can be understood as fibers developing resisting forces when shear forces in weak zones overcome soil natural shear strength [26]. In this sense, the composite reinforced with 1.4 dtex PET fibers presents a greater capacity than the composite reinforced with 3.3 dtex PET fibers.

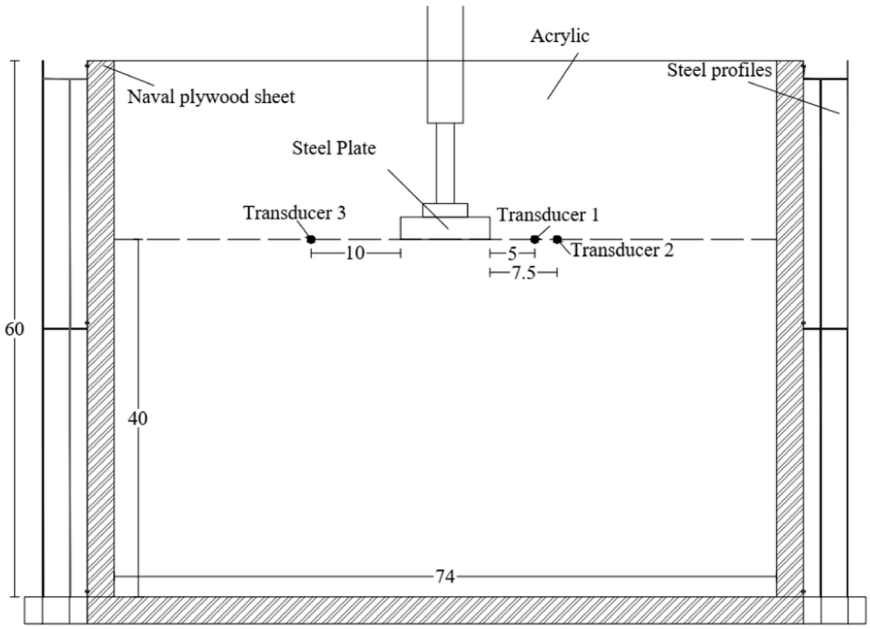

(a)

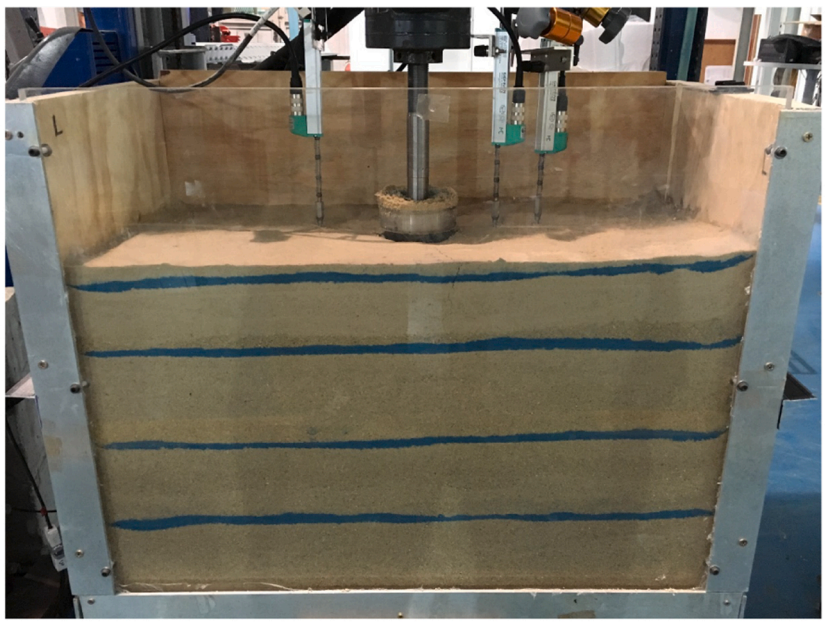

(b)

Fig. 3. Load plate test set-up: (a) cross-section; (b) overview.

3.2. Plate load tests in laboratory scale model

For the laboratory scale model tests, the 0.0098 mm diameter and 38 mm length PET fiber was utilized, based on the most efficient behavior during the triaxial tests. The load-settlement curves obtained for the sand and the sand-PET fiber composite are shown in Fig. 8.

The enhancement in the load-settlement behavior by the PET inclusion is expressed by the ability to withstand more than double the load with a lower settlement, as a result of the increased stiffness [29,38]. The behavior is attributed to the reinforcement effects,

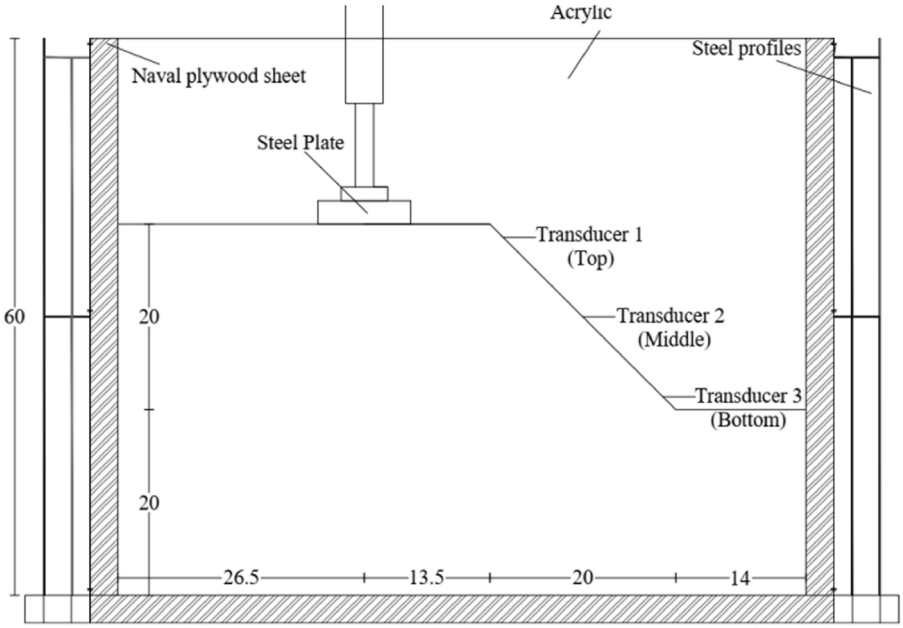

(a)

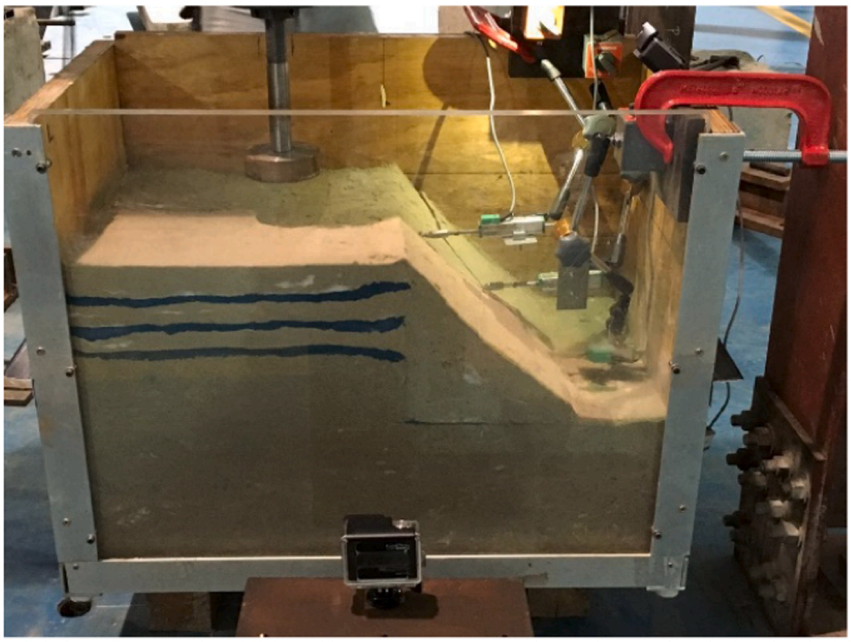

(b)

Fig. 4. Slope test set-up: (a) cross-section; (b) overview.

such as the rise in both shear strength parameters and the high degree of interlocking.

The maximum load and measured settlement obtained for the sand were 436.9 kPa and 135.6 mm, respectively, in contrast to 1141.64 kPa and 73.11 mm recorded for the sand-PET fiber composite. For the maximum comparable settlement (73.11 mm), it was seen a 375.7% enhancement in the bearing capacity.

Both materials (S100 and SF-1) demonstrated a similar path at the initial load-settlement, which is related to the sand behavior. On the other hand, the fiber inclusion begins to act together with the matrix at approximately 50 kPa, and after the S100 reaches the failure, the composite remains resisting. A nearly linear pattern could be seen during the sand-PET fiber composite test ($R^2 = 0.994$), indicating elastic behavior.

The load-settlement results present the same tendency observed by Consoli et al. [37] and Sotomayor and Casagrande [39]. In all studies, the addition of fibers, natural or synthetic, to the sandy matrix, is effective in reducing the settlements when compared to the non-reinforced soil. Moreover, the curves exhibit a similar trend when submitted to greater loads, almost parallel. Possible differences can be explained by the variability of the materials used in each work, the diameter of the plate employed, and the characteristics of the sandy soil.

It is worth noting that sand-PET behavior along the test is affected by the stress magnitude (Table 2). The waste PET fiber used in the mixture is more efficient on settlement reduction when submitted to higher loads, reaching reductions about 80% when subjected to stresses above 300 kPa. As shown by Consoli et al. [36], as well as Kumar and Kaur [56], the horizontal stresses are expected to increase under the plate during loading, increasing the confining stresses, thus, the association of continuous increase of strength at larger settlement and confining stresses lead to a stiffer response of the material. As a result, the fibers can absorb greater deformation energy and better distribute the working stresses in comparison to the unreinforced soil [38].

The settlements obtained from the displacement transducers inserted near the plate, at distances of 5 (transducer 1), 7.5 (transducer 2), and 10 cm (transducer 3) are shown in Fig. 9. For the S100, it is seen as a settlement closer to the edge of the plate, while for the distances of 7.5 and 10 cm, a raising of the sand occurred during the loading. The phenomenon characterizes a local failure, where there is the formation of a wedge at the edges of the foundation and a remarkable tendency to lift the soil around the foundation from the concentration of stress over a smaller area close to the loaded area [38]. The formation of radial and perpendicular fissures around the plate was observed during the plate load test of the sand (Fig. 10a).

In contrast, for the sand-PET fiber composite, it is possible to note that the vertical movement of the foundation is accompanied by the depression of the ground immediately below, and the penetration of the foundation occurs by vertical shearing around the foundation, while the surrounding soil practically does not participate in the process, characterizing a punching failure. Although it

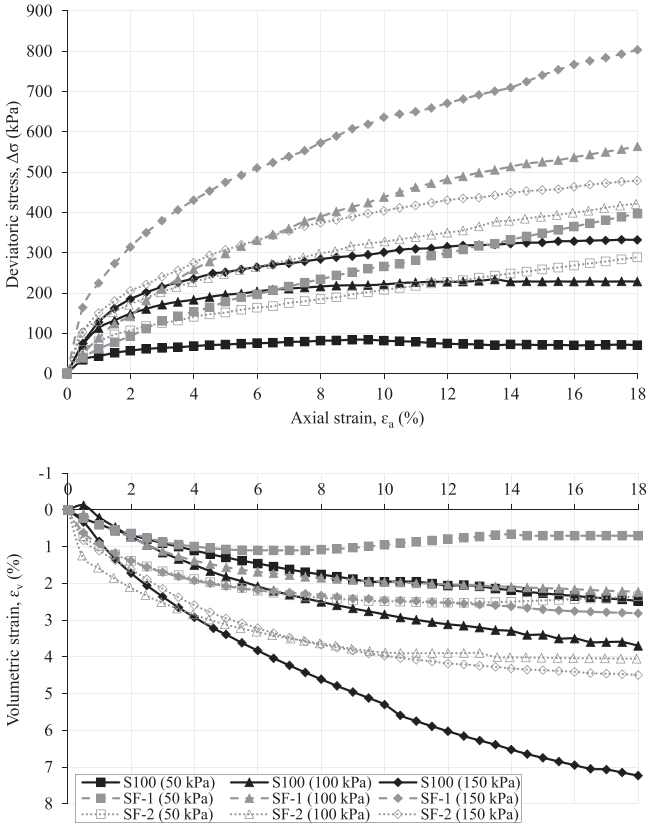

Fig. 5. Stress-strain-volumetric behavior of sand and sand-PET fiber composites in conventional triaxial compression tests.

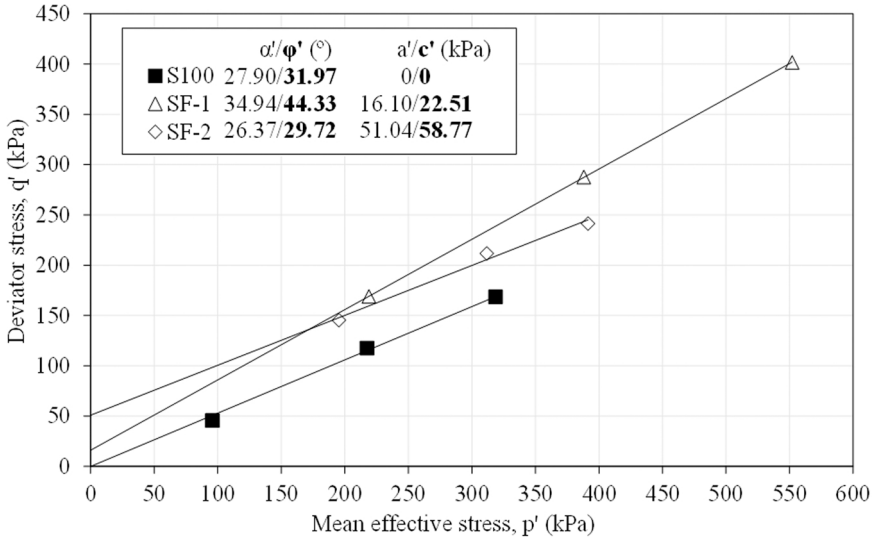

Fig. 6. Strength envelopes for sand and sand-PET fiber composites.

does not avoid the appearance of cracks, the insertion of the fiber reduces the sand movement due to its pullout resistance, controlled by the friction between the materials [53,57,58]. Moreover, the reinforcing elements can absorb greater deformation energy and distribute the generated stresses underneath the loaded area over a larger area (Fig. 10b). The satisfactory interlocking between the fibers and soil grains creates a relatively uniform strengthened composite, able to dissipate the energy under the load area [36].

The horizontal displacements measured by the transducers during the slope tests in the laboratory scale model are presented in Fig. 11. The readings obtained in the sand test at the crest were larger than the middle and base readings, which matches the rupture surface formed in the slope because, upon breaking, the soil at the top of the slope was lifted. The transducer placed at the base of the slope suffered a displacement contrary to the others because when breaking, the soil transposed the level of the transducer, precluding the actual readings.

For the sand-PET fiber composite, the displacements were significantly reduced, and the slope collapsed at higher stresses, supporting approximately three times more load than the sand performance. Comparing the displacement patterns between unreinforced and fiber-reinforced sand, the tensile restraint produced by the fibers leads to increase the effective confining pressure, which increases the frictional portion of the strength and acts by holding the soil grains from moving toward the slope face, as observed by Consoli et al. [37] and Mirzababaei et al. [38]. It is noticed that the composite slope suffered a horizontal deformation in the middle of its surface, which only begins to occur approximately at 300 kPa, approximately the same load where the sand collapses, confirming the hypothesis that when the soil no longer supports the applied loads the fibers begin to act, preventing the slope rupture.

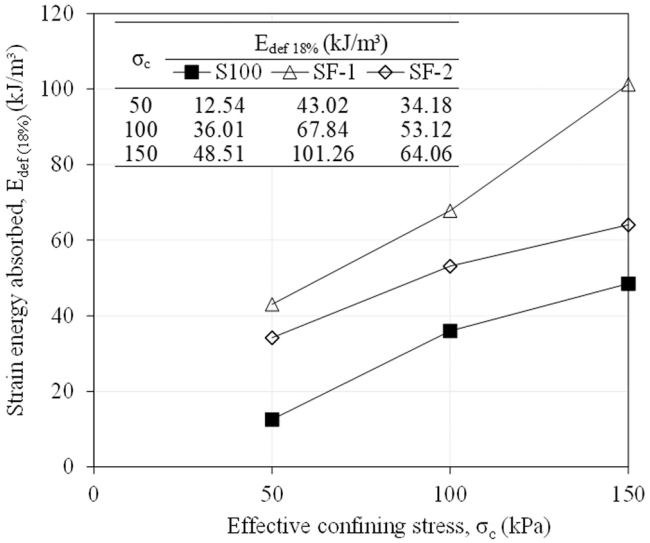

Fig. 7. Strain energies absorbed at 18% of axial strain.

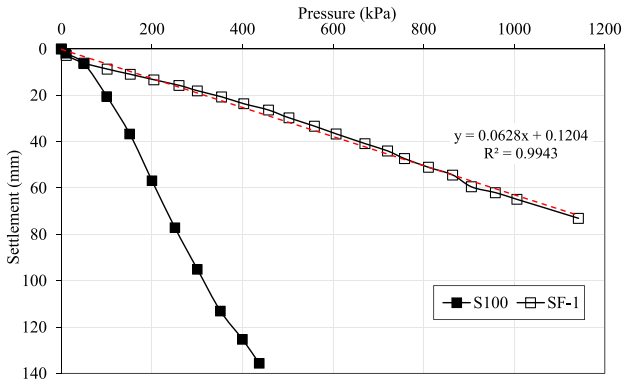

Fig. 8. Pressure-settlement behavior for non-reinforced and fiber-reinforced sand.

Table 2
Stress level effect on sand-PET fiber settlement reduction efficiency.

Stress (kPa)	Settlement (mm)		Settlement reduction (%)
	S100	SF-1	
50	6.39	6.06	5.2
100	20.47	8.68	57.6
200	56.83	13.31	76.6
300	95.15	18.05	81.0
400	125.35	23.64	81.1

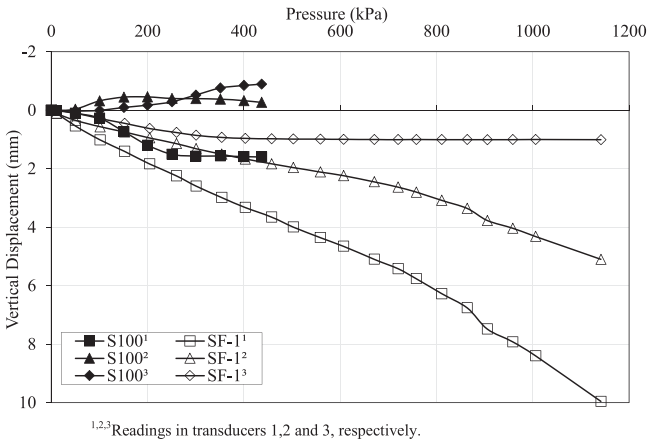

Fig. 9. Vertical displacement measured near the plate for non-reinforced and fiber-reinforced sand.

4. Concluding remarks

Based on the results and analyses presented on the paper, it is possible to conclude that:

- Both fibers improved the stress-strain behavior and absorbed strain energy of non-reinforced sand as well as increased stiffness. Superior strength parameters gains were obtained for the 1.4 dtex fiber, with the appearance of 22.51 kPa in cohesion intercept and increment of sand internal friction angle from 31.9º to 44.3º.
- PET fibers addition in the sand matrix contributes to an increase in soil strength and reduces the deformation in both vertical and lateral directions, distributing the applied stress more uniformly in a larger area. Considering the maximum comparable settlement of 73.11 mm, the bearing capacity enhanced from 240 to 1141.6 kPa.
- The settlement reduction in fiber-reinforced sand is stress-magnitude dependent. At 400 kPa, the settlement of 125.3 mm from unreinforced sand decreased to 23.6 mm by the addition of the fibers, showing a decrease of at least 80%.

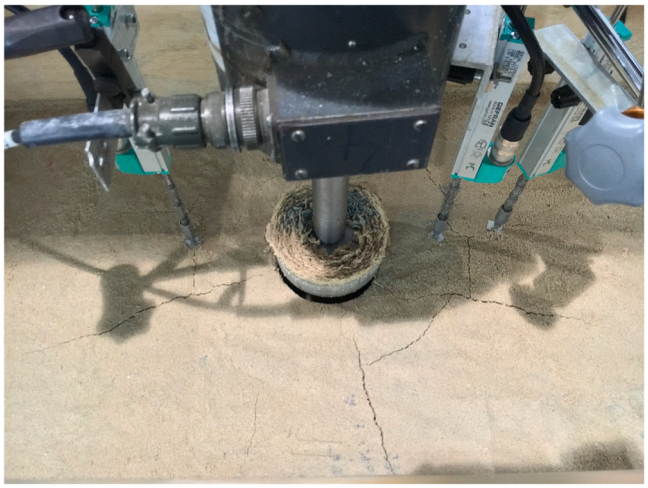

(a)

(b)

Fig. 10. Failure mechanisms obtained for (a) sand soil; (b) sand-PET fiber.

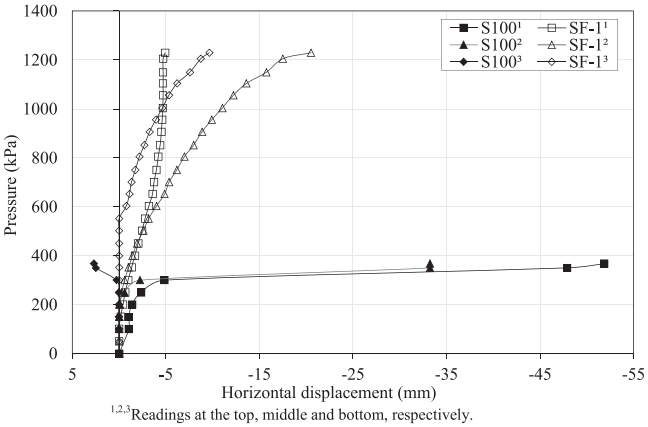

Fig. 11. Horizontal displacement for non-reinforced and fiber-reinforced sand.

- The reinforcing elements changed the soil rupture mechanism from local failure, in which occurs the concentration of stress over a smaller area close to the loaded area, to punching shear failure, wherein reinforcing elements absorb greater deformation energy and distribute the generated stresses underneath the loaded area out over a larger area.

Declaration of Competing Interest

The authors declare that they have no known competing financial interests or personal relationships that could have appeared to influence the work reported in this paper.

Acknowledgements

The authors wish to express their gratitude to the financial supports provided from Brazilian government National Council for Scientific and Technological Development (CNPq), for the Productivity Research and Ph.D. scholarships, and to the Coordination for the Improvement of Higher Level or Education Personnel (CAPES), for providing the Master scholarship.

References

[1] A. Arulrajah, E. Yaghoubi, Y.C. Wong, S. Horpibulsuk, Recycled plastic granules and demolition wastes as construction materials: resilient moduli and strength characteristics, Constr. Build. Mater. 147 (2017) 639–647, https://doi.org/10.1016/j.conbuildmat.2017.04.178.
[2] A. Edincliler, A.F. Cabalar, A. Cagatay, A. Cevik, Triaxial compression behavior of sand and tire wastes using neural networks, Neural Comput. Appl. 21 (2012) 441–452, https://doi.org/10.1007/s00521-010-0430-4.
[3] A. Mohammadinia, Y.C. Wong, A. Arulrajah, S. Horpibulsuk, Strength evaluation of utilizing recycled plastic waste and recycled crushed glass in concrete footpaths, Constr. Build. Mater. 197 (2019) 489–496, https://doi.org/10.1016/j.conbuildmat.2018.11.192.
[4] N.S.L. Louzada, J.A.C. Malko, M.D.T. Casagrande, Behavior of clayey soil reinforced with polyethylene terephthalate, J. Mater. Civ. Eng. 31 (2019), 04019218, https://doi.org/10.1061/(asce)mt.1943-5533.0002863.
[5] A.F. Cabalar, M.D. Abdulnafaa, V. Isbuga, Plate loading tests on clay with construction and demolition materials, Arab. J. Sci. Eng. 46 (2021) 4307–4317, https://doi.org/10.1007/s13369-020-04916-6.
[6] M.A. Dalhat, H.I. Al-Abdul Wahhab, K. Al-Adham, Recycled plastic waste asphalt concrete via mineral aggregate substitution and binder modification, J. Mater. Civ. Eng. 31 (2019), 04019134, https://doi.org/10.1061/(asce)mt.1943-5533.0002744.
[7] L.B. Gomes, J.M. Klein, R.N. Brandalise, M. Zeni, B.C. Zoppas, A.M.C. Grisa, Study of oxo-biodegradable polyethylene degradation in simulated soil, Mater. Res. 17 (2014) 121–126, https://doi.org/10.1590/1516-1439.224713.
[8] WWF, Solving plastic pollution: transparency and accountability. World Wide Fund, Gland, Switzerland, 2019.
[9] N. Torres, J.J. Robin, B. Boutevin, Study of thermal and mechanical properties of virgin and recycled poly(ethylene terephthalate) before and after injection molding, Eur. Polym. J. 36 (2000) 2075–2080, https://doi.org/10.1016/S0014-3057(99)00301-8.
[10] R. Navarro, S. Ferrándiz, J. López, V.J. Seguí, The influence of polyethylene in the mechanical recycling of polyethylene terephtalate, J. Mater. Process. Technol. 195 (2008) 110–116, https://doi.org/10.1016/j.jmatprotec.2007.04.126.
[11] D.H. Gray, H. Ohashi, Mechanics of fiber reinforcement in sand, J. Geotech. Eng. 109 (1983) 335–353, https://doi.org/10.1061/(ASCE)0733-9410(1983)109:3(335).
[12] N.C. Consoli, K.S. Heineck, M.D.T. Casagrande, M.R. Coop, Shear strength behavior of fiber-reinforced sand considering triaxial tests under distinct stress paths, J. Geotech. Geoenvironmental Eng. 133 (2007) 1466–1469, https://doi.org/10.1061/(asce)1090-0241(2007)133:11(1466).
[13] C.H. Benson, M.V. Khire, Reinforcing sand with strips of reclaimed high-density polyethylene, J. Geotech. Eng. 120 (1994) 838–855.
[14] A. Ahmed, Simplified regression model to predict the strength of reinforced sand with waste polystyrene plastic type, Geotech. Geol. Eng. 30 (2012) 963–973, https://doi.org/10.1007/s10706-012-9519-0.
[15] N.C. Consoli, J.P. Montardo, P.D.M. Prietto, G.S. Pasa, Engineering behavior of a sand reinforced with plastic waste, J. Geotech. Geoenvironmental Eng. 128 (2002) 462–472, https://doi.org/10.1061/(asce)1090-0241(2002)128:6(462).
[16] S.S. Park, Unconfined compressive strength and ductility of fiber-reinforced cemented sand, Constr. Build. Mater. 25 (2011) 1134–1138, https://doi.org/10.1016/j.conbuildmat.2010.07.017.
[17] B. Fatahi, H. Khabbaz, B. Fatahi, Mechanical characteristics of soft clay treated with fibre and cement, Geosynth. Int. 19 (2012) 252–262, https://doi.org/10.1680/gein.12.00012.
[18] S. Dhar, M. Hussain, The strength behaviour of lime-stabilised plastic fibre-reinforced clayey soil, Road Mater. Pavement Des. 20 (2018) 1757–1778, https://doi.org/10.1080/14680629.2018.1468803.
[19] K. Ghavami, R.D. Toledo Filho, N.P. Barbosa, Behaviour of composite soil reinforced with natural fibres, Cem. Concr. Compos. 21 (1999) 39–48, https://doi.org/10.1016/S0958-9465(98)00033-X.
[20] R. Sahu, R. Ayothiraman, G.V. Ramana, Dynamic response of model footing on hair fiber-reinforced sand, Geotech. Geol. Eng. 38 (2020) 5897–5913, https://doi.org/10.1007/s10706-020-01401-7.
[21] N. Shariatmadari, M. Karimpour-Fard, H. Hasanzadehshooiili, S. Hoseinzadeh, Z. Karimzadeh, Effects of drainage condition on the stress-strain behavior and pore pressure buildup of sand-PET mixtures, Constr. Build. Mater. 233 (2020), 117295, https://doi.org/10.1016/j.conbuildmat.2019.117295.
[22] M.V. Silveira, A.V. Calheiros, M.D.T. Casagrande, Applicability of the expanded polystyrene as a soil improvement tool, J. Mater. Civ. Eng. 30 (2018), 06018006, https://doi.org/10.1061/(asce)mt.1943-5533.0002276.
[23] K. Sobhan, M. Mashnad, Mechanical stabilization of cemented soil–fly ash mixtures with recycled plastic strips, J. Environ. Eng. 129 (2003) 943–947, https://doi.org/10.1061/(asce)0733-9372(2003)129:10(943).
[24] T. Yetimoglu, O. Salbas, A study on shear strength of sands reinforced with randomly distributed discrete fibers, Geotext. Geomembr. 21 (2003) 103–110, https://doi.org/10.1016/S0266-1144(03)00003-7.
[25] C. Tang, B. Shi, W. Gao, F. Chen, Y. Cai, Strength and mechanical behavior of short polypropylene fiber reinforced and cement stabilized clayey soil, Geotext. Geomembr. 25 (2007) 194–202, https://doi.org/10.1016/j.geotexmem.2006.11.002.
[26] M. Mirzababaei, M. Miraftab, M. Mohamed, P. McMahon, Unconfined compression strength of reinforced clays with carpet waste fibers, J. Geotech. Geoenvironmental Eng. 139 (2013) 483–493, https://doi.org/10.1061/(asce)gt.1943-5606.0000792.
[27] E. Botero, A. Ossa, G. Sherwell, E. Ovando-Shelley, Stress-strain behavior of a silty soil reinforced with polyethylene terephthalate (PET), Geotext. Geomembr. 43 (2015) 363–369, https://doi.org/10.1016/j.geotexmem.2015.04.003.
[28] N. Cristelo, V.M.C.F. Cunha, M. Dias, A.T. Gomes, T. Miranda, N. Araújo, Influence of discrete fibre reinforcement on the uniaxial compression response and seismic wave velocity of a cement-stabilised sandy-clay, Geotext. Geomembr. 43 (2015) 1–13, https://doi.org/10.1016/j.geotexmem.2014.11.007.
[29] A. Diambra, E. Ibraim, Fibre-reinforced sand: interaction at the fibre and grain scale, Geotechnique 65 (2015) 296–308, https://doi.org/10.1680/geot.14.P.206.
[30] N.R. Malidarreh, I. Shooshpasha, S.M. Mirhosseini, M. Dehestani, Effects of reinforcement on mechanical behaviour of cement treated sand using direct shear and triaxial tests, Int. J. Geotech. Eng. 12 (2017) 491–499, https://doi.org/10.1080/19386362.2017.1298300.

[31] A. Diambra, A.R. Russell, E. Ibraim, D.M. Wood, Determination of fibre orientation distribution in reinforced sands, Geotechnique 57 (2007) 623–628, https://doi.org/10.1680/geot.2007.57.7.623.
[32] E. Ibraim, S. Fourmont, Behaviour of sand reinforced with fibres, in: Soil Stress. Behav. Meas. Model. Anal., 2007: pp. 807–818. ⟨https://doi.org/10.1007/978–1-4020–6146-2_60⟩.
[33] A. Diambra, E. Ibraim, D. Muir Wood, A.R. Russell, Fibre reinforced sands: experiments and modelling, Geotext. Geomembr. 28 (2010) 238–250, https://doi.org/10.1016/j.geotexmem.2009.09.010.
[34] S.M. Hejazi, M. Sheikhzadeh, S.M. Abtahi, A. Zadhoush, A simple review of soil reinforcement by using natural and synthetic fibers, Constr. Build. Mater. 30 (2012) 100–116, https://doi.org/10.1016/j.conbuildmat.2011.11.045.
[35] S. Ghadr, H. Bahadori, Anisotropic behavior of fiber-reinforced sands, J. Mater. Civ. Eng. 31 (2019), 04019270, https://doi.org/10.1061/(asce)mt.1943-5533.0002917.
[36] N.C. Consoli, M.D.T. Casagrande, P.D.M. Prietto, A. Thomé, Plate load test on fiber-reinforced soil, J. Geotech. Geoenvironmental Eng. 129 (2003) 951–955, https://doi.org/10.1061/(ASCE)1090-0241(2003)129:10(951).
[37] N.C. Consoli, M.D.T. Casagrande, A. Thomé, F.D. Rosa, M. Fahey, Effect of relative density on plate loading tests on fibre-reinforced sand, Geotechnique 59 (2009) 471–476, https://doi.org/10.1680/geot.2007.00063.
[38] M. Mirzababaei, M. Mohamed, M. Miraftab, Analysis of strip footings on fiber-reinforced slopes with the aid of particle image velocimetry, J. Mater. Civ. Eng. 29 (2016), 04016243, https://doi.org/10.1061/(asce)mt.1943-5533.0001758.
[39] J.M.G. Sotomayor, M.D.T. Casagrande, The performance of a sand reinforced with coconut fibers through plate load tests on a true scale physical model, Soils Rocks 41 (2018) 361–368, https://doi.org/10.28927/SR.413361.
[40] ASTM C1557, Standard Test Method for Tensile Strength and Young's Modulus of Fibers, ASTM Int., 2020, 1–11. ⟨https://doi.org/10.1520/C1557–20.2⟩.
[41] ASTM D6913/D6913M, Standard Test Methods for Particle-Size Distribution (Gradation) of Soils Using Sieve Analysis, ASTM Int., 2017, 1–34. ⟨https://doi.org/10.1520/D6913–17.1.6⟩.
[42] N.C. Consoli, M.D.T. Casagrande, M.R. Coop, Performance of a fibre-reinforced sand at large shear strains, Geotechnique 57 (2007) 751–756, https://doi.org/10.1680/geot.2007.57.9.751.
[43] M. Chen, S.L. Shen, A. Arulrajah, H.N. Wu, D.W. Hou, Y.S. Xu, Laboratory evaluation on the effectiveness of polypropylene fibers on the strength of fiber-reinforced and cement-stabilized Shanghai soft clay, Geotext. Geomembr. 43 (2015) 515–523, https://doi.org/10.1016/j.geotexmem.2015.05.004.
[44] Y.W. Yoon, S.H. Cheon, D.S. Kang, Bearing capacity and settlement of tire-reinforced sands, Geotext. Geomembr. 22 (2004) 439–453, https://doi.org/10.1016/j.geotexmem.2003.12.002.
[45] K. Salimi, M. Ghazavi, Soil reinforcement and slope stabilisation using recycled waste plastic sheets, Geomech. Geoeng. 00 (2019) 1–12, https://doi.org/10.1080/17486025.2019.1683620.
[46] A.W. Skempton, The pore-pressure coefficients a and b, Geotechnique 4 (1954) 143–147, https://doi.org/10.1680/geot.1954.4.4.143.
[47] K.H. Head. Manual of Soil Laboratory Testing: Effective Stress Tests, second ed., John Wiley & Sons, England, 1998.
[48] K. Terzaghi, R.B. Peck, G. Mesri, Soil Mechanics in Engineering Practice, New York, 1996.
[49] Y. Toyosawa, K. Itoh, N. Kikkawa, J.J. Yang, F. Liu, Influence of model footing diameter and embedded depth on particle size effect in centrifugal bearing capacity tests, Soils Found 53 (2013) 349–356, https://doi.org/10.1016/j.sandf.2012.11.027.
[50] ABNT NBR 6489, Soil- Static Load Test on Shallow Foundation, Brazilian Assoc. Tech. Stand., 2019, 1–11.
[51] A.P.S. Dos Santos, N.C. Consoli, B.A. Baudet, The mechanics of fibre-reinforced sand, Geotechnique 60 (2010) 791–799, https://doi.org/10.1680/geot.8.P.159.
[52] M.H. Maher, D.H. Gray, Static response of sands reinforced with randomly distributed fibers, J. Geotech. Eng. 116 (1990) 1661–1677, https://doi.org/10.1061/(ASCE)0733-9410(1990)116:11(1661).
[53] J.G. Zornberg, Discrete framework for limit equilibrium analysis of fibre-reinforced soil, Geotechnique. 52 (2002) 593–604, https://doi.org/10.1680/geot.2002.52.8.593.
[54] K.S. Heineck, M.R. Coop, N.C. Consoli, Effect of microreinforcement of soils from very small to large shear strains, J. Geotech. Geoenvironmental Eng. 131 (2005) 1024–1033, https://doi.org/10.1061/(asce)1090-0241(2005)131:8(1024).
[55] S. He, X. Wang, H. Bai, Z. Xu, D. Ma, Effect of fiber dispersion, content and aspect ratio on tensile strength of PP fiber reinforced soil, J. Mater. Res. Technol. 15 (2021) 1613–1621, https://doi.org/10.1016/j.jmrt.2021.08.128.
[56] A. Kumar, A. Kaur, Model tests of square footing resting on fibre-reinforced sand bed, Geosynth. Int. 19 (2012) 385–392, https://doi.org/10.1680/gein.12.00024.
[57] J.D. Frost, J. Han, Behavior of interfaces between fiber-reinforced polymers and sands, J. Geotech. Geoenvironmental Eng. 125 (1999) 633–640, https://doi.org/10.1061/(ASCE)1090-0241(1999)125:8(633).
[58] C.S. Tang, B. Shi, L.Z. Zhao, Interfacial shear strength of fiber reinforced soil, Geotext. Geomembr. 28 (2010) 54–62, https://doi.org/10.1016/j.geotexmem.2009.10.001.